Molecular Dynamics of Localized Reaction, Experiment and Theory: Methyl Bromide on Si(111)-7×7

Hong Guo,[†] Wei Ji,[†,‡] John C. Polanyi[§,*] Jody (S. Y.) Yang[§]

[†]Centre for the Physics of Materials and Department of Physics, McGill University, Montréal, Québec, Canada H3A 2T8, [‡]Beijing National Laboratory for Condensed Matter Physics, Institute of Physics, Chinese Academy of Sciences, P.O. Box 603, Beijing 100080, China, and [§]Department of Chemistry and Institute of Optical Sciences, University of Toronto, 80 St. George Street, Toronto, Ontario, Canada M5S 3H6

ABSTRACT An earlier experimental study by scanning tunneling microscopy (STM) from this laboratory described the use of "localized reaction" as a means to the electron- or photon-imprinting of self-assembled patterns of CH_3Br(ad) as covalently bound Br—Si(s) at Si(111)-7×7. Here we show that the *thermal* surface bromination reaction by CH_3Br(ad) is also highly localized, and present a detailed *ab initio* dynamical model for the reaction, using DFT. Localization is seen to be due to the coexistence in the reactive transition-state of the neighboring bonds being broken (C—Br) and formed (Br—Si). Both experiment and theory are consistent with a low energy-barrier, $E_a \approx 0.2$ eV, for the thermal bromination of Si(111) by CH_3Br(ad), and also for the desorption of intact CH_3Br(g) ($E_{des} \approx 0.2$ eV). Two physisorbed states of CH_3Br(ad)/Si(111) (I and II) are distinguishable by STM at 50 K by their differing displacement from the underlying Si adatom. These states can be identified with similarly displaced states in the STM images simulated by DFT. At the elevated temperature of 80 K, a markedly displaced physisorbed state (III) appears in the STM image, indicated by DFT to have a configuration encountered along the reaction path immediately prior to the transition state. The electron-induced bromination of Si(111) by CH_3Br(ad), and also electron-induced molecular desorption, are examined as a function of the energy of the incident electron, giving for both processes a threshold energy of $E_e \approx 1.8$ eV in accord with *ab initio* theory, and a substantial yield of 10^{-6} to 10^{-5} Br—Si(s)/electron.

KEYWORDS: reaction dynamics · thermal reaction · electron-induced reaction · methyl bromide · Si(111)-7×7 · STM · DFT

The study of molecular motions in chemical reactions, reaction dynamics, is a mature field in gases[1] but an emerging field at surfaces where scanning tunneling microscopy (STM) offers the possibility of studying the dynamics one molecule at a time.[2]

This fundamental area of study has clear practical importance. The first step in nanofabrication at surfaces is necessarily the self-assembly of mobile physisorbed species.[3–6] To be useful self-assembled structures will, however, in general need to be stabilized[7] which may be achievable by chemical binding to the underlying surface. This can, in principle, be induced by heat, light, or electrons. So that a transition from physisorption to chemisorption does not destroy the self-assembled pattern, this induced reaction must be highly localized adjacent to the physisorbed adsorbates by means of a "localized reaction".[8,9]

In an earlier study of the title reaction,[10]

$$CH_3Br(ad)/Si(111)\text{-}7\times7 \rightarrow CH_3(g) + Br{-}Si(111)\text{-}7\times7 \quad (1)$$

it was shown that both photon-induced and electron-induced reaction could convert a physisorbed pattern into an identical chemisorbed pattern, that is, the surface bromination of Si(111)-7×7 was localized to the position of the prior physisorbed parent molecule, CH_3Br(ad). It was suggested on the basis of a simple model[10] that the electron-induced reaction occurred in both cases by electron-transfer to the CH_3Br(ad) followed by downward recoil of Br^- toward the surface, and its localized capture at the nearest Si-atom to form neutral Br—Si due to efficient reverse electron-transfer to the substrate.

In the present study we have extended our investigation of "localized atomic reaction" (LAR)[10] to the case of thermal (rather than photon- or electron-induced) reaction (1), which is shown to occur readily at ~60 K over a low activation barrier. Since the thermal reaction can be pictured as occurring on a single ground-state electronic potential-energy surface we have been able for the first time to make an extensive *ab initio* study of the molecular dynamics of the Br-atom transfer from physisorbed CH_3Br(ad) to a chemisorbed state at the underlying Si(111)-7×7 surface. Details of both experiment and theory are presented here for the first time. The high-degree of localization of the Br—Si to the neighborhood of the parent CH_3Br(ad) molecule is shown to be due to the concerted nature of

*Address correspondence to jpolanyi@chem.utoronto.ca.

Received for review January 10, 2008 and accepted March 03, 2008.

Published online April 4, 2008.
10.1021/nn800017d CCC: $40.75

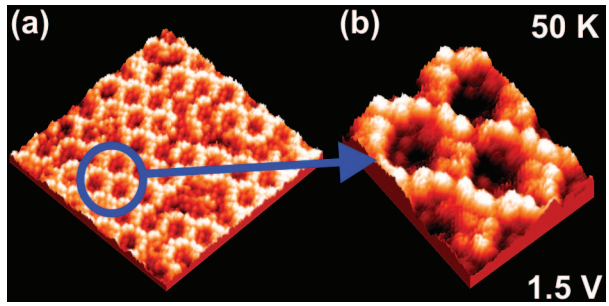

Figure 1. STM images of physisorbed CH_3Br (V_s = 1.5 V, I_t = 0.2 nA, ~140 × 190 Å^2) and close-up of three circles, each individual circle consisting of 12 physisorbed CH_3Br (V_s = 1.5 V, I_t = 0.2 nA, ~40 × 40 Å^2) at 50 K.

the reaction, which necessitates that the original molecular site of the Br in the parent molecule CH_3Br(ad) be closely adjacent to its final site chemically bound to the underlying Si-adatom.

Additionally we have quantified our earlier report of the localized electron-induced bromination of the same surface in reaction (1)[10] by measuring the threshold energy E_e and electron-yield, Y, of the reaction. Electron-induced reaction under the STM tip is presently an active field of study.[11−20] Theory, presented here, shows that this threshold energy, measured for the first time for the title reaction, correlates with the energy of the lowest unoccupied molecular orbital (LUMO) of physisorbed CH_3Br(ad)/Si(111)-7×7. The implications of the very large electron-yield for this process are noted.

RESULTS AND DISCUSSION

Physisorption. ***Experiment.*** Figure 1a shows the characteristic circles of diffuse features corresponding to physisorbed intact methyl bromide adsorbed on middle adatoms of Si(111)-7×7 at 50 K. From previous work the bright features in the STM trace of Figure 1 are identified as being physisorbed intact methyl bromide molecules.[10] Methyl bromide physisorbs preferentially on Si middle-adatoms at 50 K.[10] With the approximate 0.5-monolayer (ML) surface coverage almost all Si middle-adatoms are occupied by physisorbed methyl bromide, forming bright conjoined-circles. Figure 1b gives a close-up of three such circles, each consisting of 12 physisorbed methyl bromide molecules.

A close examination of 100 physisorbed molecules made in this study revealed for the first time that at 50 K the methyl bromide could adopt two physisorbed configurations (termed I and II). Figure 2a shows that configurations I and II are characterized by being 0.3 and 0.7 Å displaced laterally from the underlying Si-adatom at peak, respectively. The location of the Si middle-adatoms was calculable from the position of the neighboring adatoms. Upon annealing to 80 K, a (different) area of 87 physisorbed molecules was examined. This revealed a third physisorbed configuration III of the methyl bromide in addition to I′, together with the disappearance of configuration II, as shown in Figure 2b. Configuration III is the most substantially laterally displaced from the underlying Si middle-adatom, by 1.2 Å. These will be discussed from the standpoint of *ab initio* theory later.

The STM images in the inset to Figure 2 panels a and b show that the physisorbed molecules appear less diffuse in panel b, indicating increased stability in the physisorbed molecules at 80 K, comprising 90% configuration I′ (indistinguishable in lateral displacement from I) which therefore gives evidence of being more resistant to lateral displacement at the surface (see later). Since there is some interaction between adjacent physisorbed molecules, increased surface-binding for I′ will serve to stabilize the minority in III.

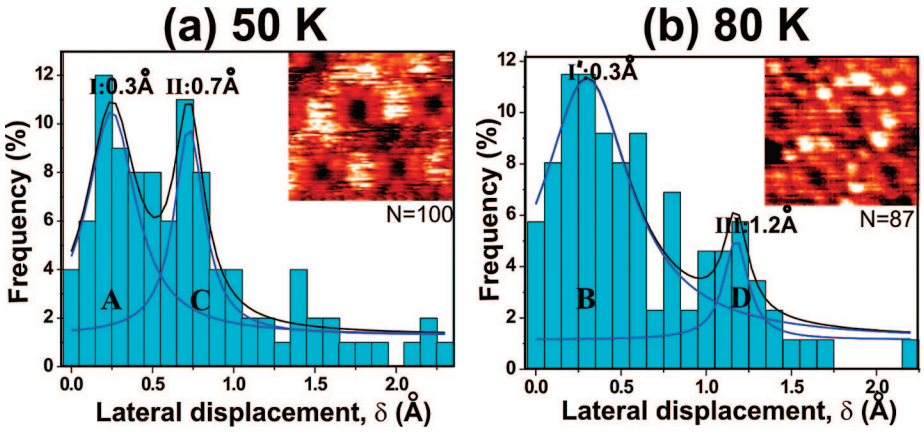

Figure 2. Physisorbed CH_3Br distribution relative to the lateral displacement from the underlying Si and corresponding STM images (V_s = 1.5 V, I_t = 0.2 nA, ~60 × 60 Å^2), obtained at (a) 50 K and (b) 80 K. (a) At 50 K, two configurations, I and II, are found 0.3 (measured value of 0.25 ± 0.02) and 0.7 (measured value of 0.72 ± 0.02) Å displaced from underlying Si, respectively. (b) At 80 K, configuration III appears 1.2 (measured value of 1.17 ± 0.05) Å displaced from underlying Si, in addition to configuration I′ (same peak position as I). The letters A−D correlate the experimentally observed peaks with theory. The insets in panels a and b show typical STM images of physisorbed CH_3Br(ad) obtained at 50 and 80 K.

Theory. Plane-wave-based density functional theory (DFT) total energy calculations were employed to search for stable physisorbed structures. We started from 16 different initial configurations and by minimizing the total energy obtained the three different structures, **A**, **C**, and **D**, shown in Figure 3a,c,d together with corresponding simulated STM images. A fourth configuration, **B**, shown in Figure 3b, was identified during the reaction-coordinate search. A difference between theoretical structures **A** and **B**, in addition to the fact that **B** has its C−Br bond more-tilted toward the surface, is that the molecule has shifted laterally: in **A** the C and Br atoms are on the

same side of the Si middle-adatom, whereas in **B** they are on opposite sides of this Si. The lateral displacement of the CH_3Br(ad) from the underlying Si atom in **A** and **B** can be determined from the simulated STM images (Figure 3) to be 0.36 and 0.38 Å, respectively. These two lateral displacements are consistent with the STM measured value of 0.3 Å for both configuration I and I′. Since **A** is observed to move more readily away from its equilibrium position than **B** and **A** appears to have a lower force-constant for displacement from its equilibrium location than **B** (see thermal reaction theory, later), we tentatively attribute theoretical structure **A** to the observed peak I at 50 K and **B** to the peak I′ at 80 K in which the images are sharper.

Theoretical structure **C** in Figure 3c is displaced by 0.75 Å laterally from the on-top site of the Si middle-adatom. This is in good agreement with the measured 0.7 Å lateral displacement for configuration II (Figure 2a) with which we, therefore, identify structure **C**. Computed structure **D** (Figure 3d) has a simulated image which is displaced by 0.93 Å from the underlying Si middle-adatom. We identify structure **D** with the experimental configuration III observed only at the higher temperature of 80 K (Figure 2b) which has a measured displacement of 1.2 Å. Structure **B** and **D** (but not **C**), as will be shown, closely resemble configurations encountered along the reaction coordinate, structure **D** being close to the computed reactive transition state.

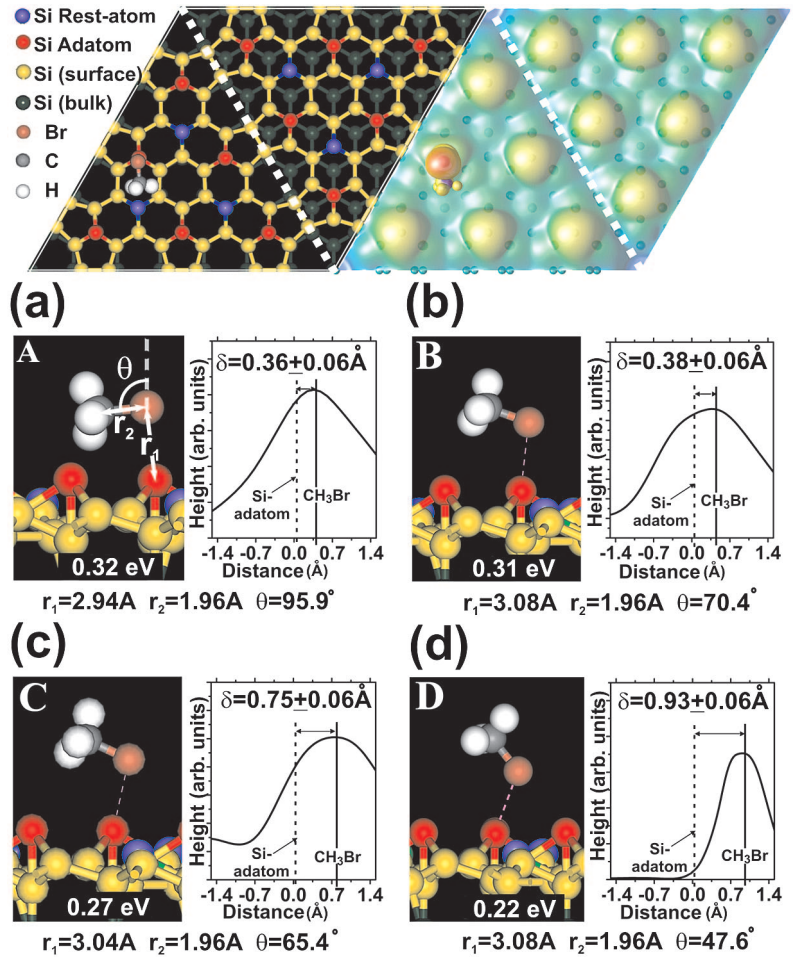

Figure 3. Theory. (Top view, above) Real-space model (left) and simulated STM image (right) of calculated structure of CH_3Br on Si(111)-7×7 unit-cell. The calculated STM image at the right is shown with the surface bias of 1.5 V. The colors indicate the height of the images, blue being low and red being high. (Side views, a, b, c and d below) Computed meta-stable structures A−D and height profiles of CH_3Br(ad)/Si indicating the lateral displacement, δ, of CH_3Br with respect to the underlying Si. Structures A, B, C, and D are thought to correspond to configurations I (a), I′ (b), II (c), and III (d), respectively. The adsorption energy, distance between Br and Si, r_1, bond length between C and Br, r_2, and the angle, θ, between CH_3Br and the surface normal, are shown.

Thermal Reaction. ***Experiment.*** The experiments showed no measurable thermal reaction at the temperature of 50 K used in recording both Figure 1 and Figure 2a. Thermal reaction to brominate the surface took place at an observable rate at temperatures in excess of 55 K. (The data of Figure 2b presented earlier, regarding the physisorbed configurations present at 80 K, were taken from a single STM scan at 80 K; the few reacted molecules were not included in the figure which gives only the configurations of the physisorbed molecules at this temperature.)

A measurement was made of the rate of thermal reaction at 57 K by scanning at uneven intervals and counting the number of reacted molecules as a function of time at intervals of minutes. Figure 4a recorded at 80 K (1.5 V) shows an almost complete-circle of physisorbed CH_3Br at the right of panel a, and panel b shows the same area after 20 min, at which time localized thermal reaction has given rise to a similar circle of chemisorbed Br-atoms (dark at 1.5 V). The characteristic "lighting-up" effect on chemisorbed Br (*i.e.*, Br−Si) of increasing the surface bias from 1.5 to 2.5 V,[10] is shown in Figure 4d as compared with 4c. The fact that Br is chemisorbed as Br−Si is also evidenced by its long-term stability at room temperature following many hours, since the physisorbed species would desorb at >80 K. The localization of reaction is evidenced by the formation of circles of chemisorbed Br atoms (Br−Si) which are shown to derive from the prior presence of physisorbed circles at the surface.

To measure the reaction rates, some 264 physisorbed molecules were followed over time; 44 were observed to react over a period of 20 min. A record was also kept of the decreasing total number of physisorbed plus reacted molecules remaining as a function of time and hence the number desorbed (42) over this same period. The rate constants for the two processes, reaction and desorption, were both $k = 4 \times 10^{-4}$ sec^{-1}. The Arrhenius activation energy, assuming a pre-

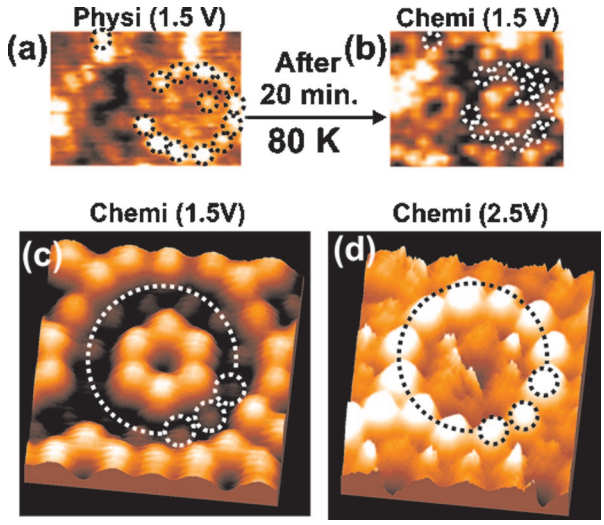

Figure 4. STM images showing (a) physisorbed CH_3Br(ad) at 80 K (indicated by broken circles) and (b) the same area 20 min later with localized reaction as indicated (V_s = 1.5 V, I_t = 0.2 nA, 54 × 56 Å^2). Panels c and d show different parts of the surface. In panel c a chemisorbed circle is shown after warming to room temperature (~100% thermal reaction) consisting of 12 Br (3 are indicated by broken circles which somewhat obscure the image, the remaining 9 are indicated by a dashed line to avoid obscuring their images), scanned at (c) 1.5 V at left and (d) 2.5 V at the right (I_t = 0.2 nA, 28 × 28 Å^2).

exponential factor of $A = 10^{13}$ s^{-1},[21,22] is $E_a \approx 0.2$ eV for the thermal bromination reaction and also $E_{des} \approx 0.2$ eV for desorption of intact methyl bromide.

It is noteworthy that the only processes observed at 57 K were formation of Br−Si (by thermal reaction) and desorption of intact methyl bromide (thermal desorption). No residual hydrocarbon (CH_3−Si) was observed from the thermal reaction. In previous work with long-chain alkyl halides, RX(ad) on the same substrate, R-Si at the surface evidenced itself as dark features.[23,24] We conclude that if, as in the present case, R is a methyl radical, CH_3, it leaves the surface as CH_3(g).

Theory. The reaction path, which plays a key role in understanding the localized reaction, was searched theoretically using the nudged elastic band (NEB) method with "modified climbing-image"; it is shown at 10 steps in Figure 6.[25] Three final states were employed in the NEB method to explore the transition state: (i) the methyl radical was laterally displaced from the initial ground state; (ii) the methyl radical was vertically displaced with the C atom of CH_3 remaining directly above a Si adatom; (iii) the methyl radical escaped from the surface at an angle. All three calculations gave the *same* tilted configuration (panel 7 in the Figure) for the highest energy transition-state in the transfer of Br from CH_3Br to a Si middle-adatom.

All the NEB calculations converged on the same thermal reaction mechanism shown in Figure 6; there we picture the successive stages of the reaction in which the methyl radical finally escapes from the surface vertically. As illustrated by these animations, the horizontal CH_3Br in the physisorbed configuration previously designated as **A** transforms in 1–4 into a metastable configuration resembling **B**. Next (in configurations 5–7) the C−Br bond extends with the expenditure of ~0.3 eV of energy, partially transferring Br from C to Si. In the transition state (Figure 6, panel 7, designated as ‡) the charge in the "old" bond responsible for binding the C to the Br initially has been depleted as the bond extends from 1.56 to 3.19 Å. Concurrently the charge in the "new" bond binding Br to Si has increased, resulting in a decrease from its initial weakly physisorbed separation of 2.94 Å, to approximately the Br−Si covalent equilibrium separation of 2.2 Å. The compact transition state is indicative of the coexistence of the old and new bonds.

In the final stages of reaction there is evidence of a weak attraction between the methyl and the bromine. For positions 7–9, due to the tilting of the CH_3 radical to

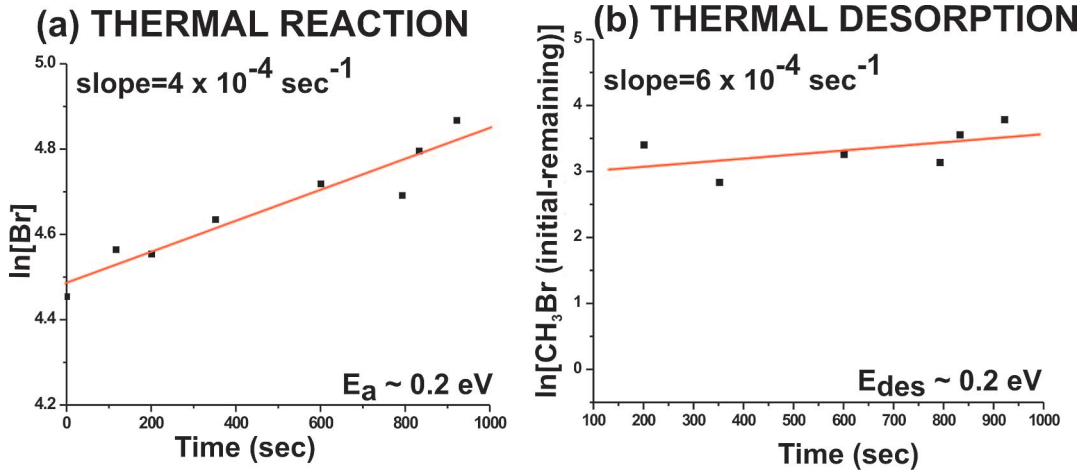

Figure 5. Plots showing (a) the increase in the number of chemisorbed Br due to thermal reaction and (b) the increase in the number of desorbed CH_3Br (observed as decrease in CH_3Br(ad)) due to thermal desorption of physisorbed CH_3Br with time at 57 K: 44 Br imprints and 42 desorbed CH_3Br were observed for thermal reaction and desorption, respectively. Both E_a(reaction) and E_{des}(desorption) were determined to be ~0.2 eV, assuming the pre-exponential factor of 10^{13} s^{-1}.

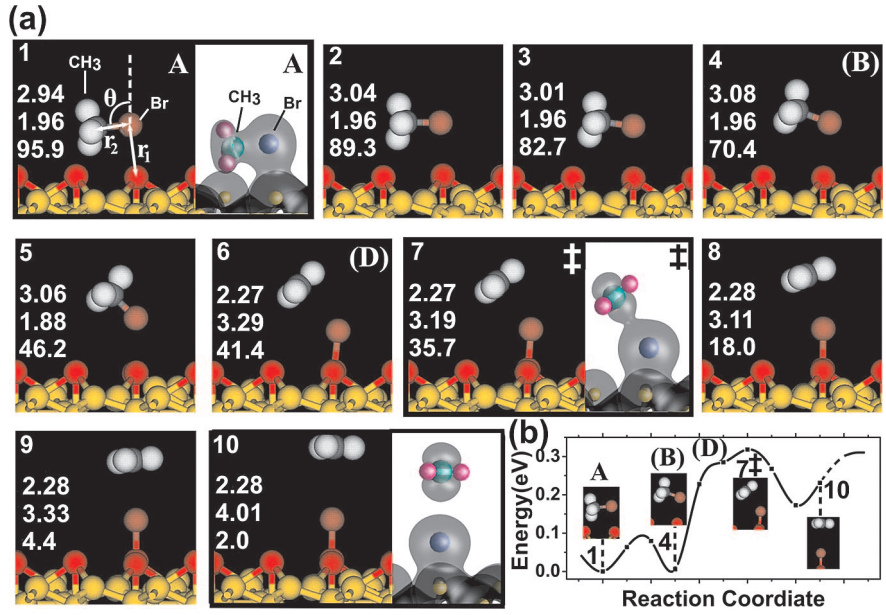

Figure 6. DFT calculation of the stages of localized surface-bromination of Si(111) by methyl bromide (methyl at left, Br at right in 1). (a) Side views of the thermal reaction path and (b) energies along this reaction path. The charge densities are shown for configurations 1, 7, and 10 by isosurface contours set to 0.05 e/Å^3. The distance between Br and Si, r_1, bond length between C and Br, r_2, and an angle between CH_3Br and the surface normal, θ, are shown superimposed on the ten successive side-views of molecular configurations. The energy profile in panel b has insets indicating four representative configurations corresponding to position 1 (physisorbed state A), position 4 (approximating physisorbed state B), position 7 (the transition state), and position 10. Position 6 corresponds approximately to physisorbed state D. The computed activation barrier for thermal reaction, with its crest at position 7 (the transition state ‡), is 0.32 eV.

a horizontal plane, the calculation shows charge-transfer from the Br of Br−Si into the C dangling bond, accounting for the weak binding of CH_3 to the surface. A further expenditure of ~0.15 eV of energy releases CH_3(g).

The calculated reaction barriers by NEB using the three final states (i−iii) mentioned above were similar; 0.31, 0.32, and 0.34 eV, respectively. The barrier-height in the reaction path illustrated in Figure 6b, computed by NEB with final state ii is 0.32 eV. Such a low reaction barrier is consistent with an observable reaction rate at low temperatures >55 K. From the small theoretical adsorption energies in Figure 3 it is evident that the energy required for the competing process of desorption is predicted to be of a similar magnitude to that required to overcome the barrier to endoergic reaction. This accords with the fact that the experimental reaction and desorption rates were roughly equal; using a pre-exponential factor of $A = 10^{13}$ s^{-1}, the barrier-height obtained was $E_a \approx 0.2$ eV for both processes, in satisfactory accord with the computed value of 0.32 eV for the barrier to reaction.

Electron-Induced Reaction. ***Experiment.*** The surface-bromination reaction and also the desorption of intact methyl bromide can be induced not only thermally but also by incident electrons from the STM tip at 50 K (at which temperature there is no *thermal* reaction or desorption.). To obtain the thresholds and yields of these electron-induced processes, physisorbed methyl bromide was scanned at various scanning biases at a measured tunneling current.

The electron yield of reacted or desorbed molecules was obtained from the dose, *D*, of electrons per molecule in the course of a scan ($D = 10^5$ electrons/molecule, for a tunneling current of 0.2 nA and an estimated time of $\sim 1 \times 10^{-3}$ s spent by the tip over a single molecule). The yield per electron, *Y*, was calculated by counting the fraction of molecules reacted or desorbed after a scan at a selected bias, divided by the dose, *D*. Figure 7 panels a and b show the electron-induced reaction yield and the electron-induced desorption yield as a function of the surface voltage. A threshold was observed in each case at which the yield increased from $\sim 10^{-6}$ to $\sim 10^{-5}$. The same threshold voltage of 1.8 V was obtained for both the reaction and desorption, assuming a linear-threshold law.[17,26]

The similar thresholds suggest that we are dealing here with the same electronic excitation. The high yields suggest a resonant transition. Since electron transfer occurs from the tip to the physisorbed methyl bromide, the electron must enter the LUMO of the adsorbed molecule. The methyl bromide anion initiates a process of surface bromination or molecular desorption which is completed on the ground-state potential following electron-transfer to the surface.

Several earlier examples of electron-induced reaction and desorption under an STM tip have been referred to in the introduction. Alavi *et al.*[12,13] explained their observations of electron-induced desorption of benzene from Si(100) by way of benzene cation formation in transient ionization, much as in the present work. They reported a high yield of $Y \approx 10^{-6}$ for

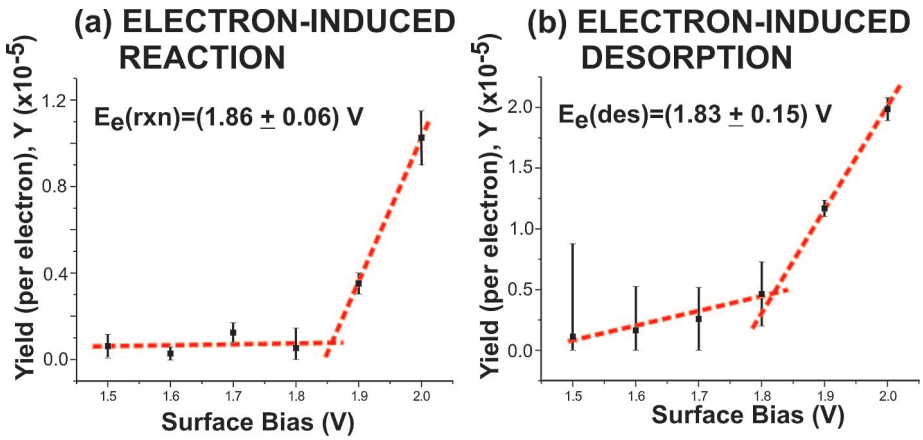

Figure 7. Electron-induced reaction or desorption yield, *Y* (per electron), of physisorbed CH_3Br(ad) on Si(111)-7×7, respectively, to give chemisorbed Br or gaseous CH_3Br, is given as a function of the surface bias at 50 K. The threshold energy E_e= 1.8 V was obtained for both processes. No detectable reaction or desorption was observed when the surface was scanned with negative surface biases up to − 2.5 V. This will be discussed in terms of *ab initio* theory later.

desorption.[12,13] The observed threshold for benzene desorption[12,13] coincided approximately with the HOMO of the adsorbed molecule. Surprisingly, in the present case electron attachment to CH_3Br gives an order of magnitude greater yield for both the reactive and desorptive pathways than was obtained for benzene desorption,[12,13] despite the lack of low lying π-states in the present case. This implies highly efficient reaction and desorption of CH_3Br^- at Si(111), probably reflecting the low energy-barrier to both processes.

M. Kawai's laboratory,[19] using STM, measured the threshold energy for the electron-induced dehydrogenation of benzene at Cu(100) with $Y = 10^{-9}-10^{-8}$, and found it to coincide with the energy of the LUMO π*-state. Dujardin and co-workers[18] have detailed, again by STM, a switching movement of biphenyl at Si(100) through the withdrawal of an electron from occupied states π1 and π2 ($Y \approx 10^{-9}$). Most recently Hersam, Seideman, and co-workers[20] reported desorption of cyclopentene from Si(100) under an STM tip, by both positive- and negative-ion formation at the surface; the threshold energies correlated with those of the HOMO and LUMO states, respectively ($Y \lesssim 10^{-9}$). The efficiencies of all these processes was 3–4 orders-of-magnitude less than those reported here. This may be related to the fact that the energy-barriers on the ground-state potential-energy surface were >1 eV as compared with only ~0.2 eV here.

Theory. We first illustrate the calculated projected density of states (PDOS) of CH_3Br−Si(111)7×7, as shown in Figure 8. The DOS is projected over each atom. The features designated Si and Si surface state (SS) in Figure 8 represent the bare Si adatom and the highest surface state of Si(111) 7×7, respectively. The antibonding state, CBr*, (the lowest unoccupied molecular orbital of CH_3Br) between C and Br is located at 2.18 eV above the Fermi level. A BrSi hybrid antibonding state, BrSi*, is at 0.37 eV above the Fermi level. The corresponding bonding state of BrSi is roughly at 2.5 eV below the Fermi level, while the corresponding bonding state of CBr is not in the energy window from −3.0 to +3.0 eV.

An electron injected by STM can enter two possible states, as follows. An electron injected into the CBr antibonding state (CBr*) is likely to weaken the C−Br bond and gives rise to an electron-induced reaction. An electron injected into the BrSi antibonding state (BrSi*) would be expected to diminish the bonding between Br and Si atoms, resulting in desorption of CH_3Br from the surface if there is a change in equilibrium BrSi separation in going to the anion state. Experimentally, at the threshold energy of E_e = 1.8 V, both reaction and desorption are induced by incident electrons from STM with high yields. This threshold electron-energy is approximately 0.4 eV lower than the energy of CBr*. The lowered threshold is explained as follows.

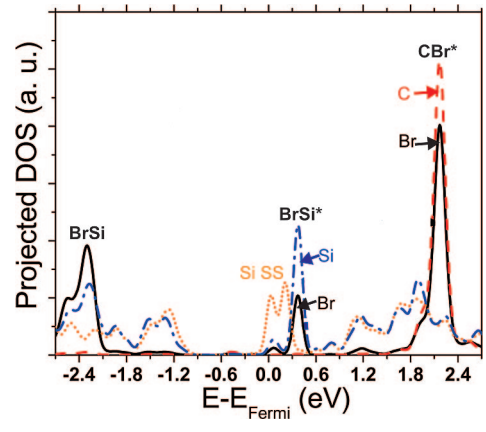

Figure 8. Projected density of states (PDOS) of CH_3Br/Si(111)7×7. The PDOS of Br (solid black line), C (dashed red line), the surface states of Si(111)-7×7, Si SS (dotted orange line), and Si-adatom reacted with CH_3Br (blue dashed-dot line) are shown. The PDOS peak at –2.31 and 0.37 eV are the Br−Si bonding (BrSi) and antibonding states (BrSi*), respectively. The large peak at 2.17 eV is the CBr antibonding state (CBr*). Its bonding state (CBr) is out of the energy range of this plot. To correspond to the experiments, the Fermi level needs to be shifted upward by ~0.4 eV to allow for the n-doping of the Si crystal.

The silicon surface modeled in our calculation is an intrinsic surface without any doping. However, the silicon wafer used in the experiment is an n-doped wafer in which the Fermi level is displaced upward. This shift will reduce the observed threshold energy. A shift of ~0.4 eV is a typical energy-shift due to band-bending in a doped silicon surface.

Electron-induced reaction by withdrawing electrons from the surface was also considered. From the PDOS plot in Figure 8, the bonding state of CBr is out of our energy-window. It follows that reaction is unlikely to be induced by withdrawing electrons from the surface using a bias voltage less than negative 3.0 V, nor was any induced reaction observed. The absence of observed desorption, though the BrSi bonding state at −2.3 eV lies within our energy-window, would be explained (according to the Menzel, Gomer, Redhead model[27,28]) if the excited-state had its potential minimum directly above that in the ground state, resulting in a minimal impulse along the BrSi coordinate.

CONCLUSION

The experiments reported here have shown for the first time that the thermal reaction of physisorbed CH_3Br(ad) to brominate an underlying Si(111)-7×7 surface giving Br−Si, is localized to the Si-adatom at which the parent molecule was physisorbed. An *ab initio* simulation of the same reaction by DFT on a 4-layer-deep slab of 200 Si atoms showed a similar localization of the chemisorbed reaction-product Br−Si at the prior site of the physisorbed reagent molecule. Theory showed that this localized reaction is due to the fact that a low energy reaction-barrier is achieved through the concurrent presence of the old chemical bond which is being broken (namely C−Br) together with the new bond being formed (Br−Si). This concerted reaction is only possible if the old and new bonds are closely adjacent, that is, if the reaction is localized. Accordingly, we would expect localization of the thermal reaction to be a general phenomenon. So that the thermal reaction shall predominate, it must have a lower energy-barrier than that for desorption or diffusion. Thermal reaction should, in selected cases, provide a means to the permanent "imprinting" of physisorbed patterns at surfaces in the chemisorbed state. Where, as is the case here, thermal desorption competes with localized thermal reaction, a complete imprinted-pattern will be obtainable by successive cycles of physisorption followed by thermal reaction. This expedient was used in earlier work on an electron-induced reaction.[10]

Experiment and theory are in accord in yielding a value of $E_a \approx 0.2$ eV for this thermal bromination reaction, $CH_3Br(ad)/Si(111) \rightarrow CH_3(g) + Br{-}Si(111)$, as well as for desorption of intact $CH_3Br(g)$ ($E_{des} \approx 0.2$ eV). The computed reaction path begins with the physisorbed molecule having its CBr axis approximately horizontal, $\theta = 96°$ from the surface normal, and then tilting upward to $\theta = 36°$ in the transition state while the bond to be broken is weakened, but not severed, extending from its equilibrium value of $r_2 = 1.96$ Å to $r_2(‡) = 3.2$ Å in the transition state.

Close examination by STM revealed four physisorbed molecular states. States I and II at 50 K were laterally displaced by 0.3 and 0.7 Å from the underlying adatom, and states I′ and III at 80 K by 0.3 Å (as in I) and 1.2 Å; states I and I′ differed in that the former gave a diffuse image the latter a sharp one. These four physisorbed states were tentatively identified with four computed states, **A**−**D,** for the intact molecule. Three of these computed states (**A**, **B**, and **D**) lay approximately along the minimum-energy path (*i.e.*, along the reaction coordinate). Observation of these differing physisorbed states offers the possibility, for the first time, of studying spontaneous or electron-induced reaction (see later) starting at various stages en route to the transition-state configuration.

The same surface-bromination reaction of CH_3Br at Si(111) could be induced by electron impact. The yield of Br−Si reaction product and also of electron-induced desorption of intact $CH_3Br(g)$ was measured as a function of the energy of the incident electron, giving for both processes a threshold of $E_e \approx 1.8$ eV in accord with *ab initio* theory, and a substantial yield of $Y = 10^{-6}{-}10^{-5}$/electron as would be expected for resonant transition into an unoccupied molecular orbital. Taking into account the effect of n-doping in shifting the Fermi level by ~0.4 eV, the measured threshold energy of $E_e \approx 1.8$ eV for both reaction and molecular desorption agrees with the value computed here for the antibonding LUMO of CBr* at approximately 2.2 eV.

METHODS

Experiment. The experiments were performed with an Omicron variable temperature STM system with base pressure $<1 \times 10^{-10}$ mbar. Methyl bromide was introduced into the UHV chamber by background dosing at 50 K. The STM was operated in constant current (0.2 nA) mode with the tunneling bias of 1.5 V at the sample. In this condition, the adsorbate/surface structure could be probed without causing any detectable reaction or desorption. Clean Si(111)-7×7 surfaces were prepared by heating the sample (phosphorus-doped, n-type, 1×9 mm^2, 250 μm thickness, 0.02–0.05 Ωcm) to ~1500 K for 100 s, at which the chamber pressure was kept under 2×10^{-10} mbar. STM tips were electrochemically etched from 0.38 mm polycrystalline tungsten wire in 2.0 M NaOH solution. Methyl bromide (gas) was purchased from Aldrich and used without further purification. To image the adsorbate/surface at 80 K, the adsorbate/surface temperature was increased at a rate of ~3 K/min. STM images were obtained 20 min after reaching 80 K to minimize thermal drift. Some reactions were observed while heating to 80 K.

Theory. The calculations were carried out using DFT, the Perdew−Burke−Ernzerhof (PBE)[29] generalized gradient approximation (GGA) for exchange-correlation potentials, the projector

augmented wave (PAW) method,[30] and a plane wave basis set as implemented in the Vienna ab initio simulation package (VASP).[31,32] For calculation of $CH_3Br-Si(111)$-7×7 system, the four layers of Si atoms and a 7 × 7 supercell were employed to model the slab. The molecule was put on only one side of the slab, while 49 H atoms are included to passivate the dangling bonds at the bottom of the surface slab. Only one Γ point was used for sampling the surface Brillouin zone for the large supercell. The energy cutoff for the plane waves was up to 400 eV. All calculations were performed applying spin-polarization. In structure relaxation, all atoms except for the bottom two silicon layers were fully relaxed until the net force on every atom was less than 0.02 eV/ Å. The potential energy profile along the reaction path was calculated using the nudged elastic band technique with a modified climbing-hill method which gives the exact saddle point of a reaction.

Acknowledgment. The authors are indebted to the Natural Sciences and Engineering Research Council of Canada (NSERC), Photonics Research Ontario (PRO; and Ontario Centre of Excellence), the Canadian Institute for Photonic Innovation (CIPI), and the Canadian Institute for Advanced Research (CIFAR) for their support. W.J. wishes to thank Prof. H. J. Gao and Institute of Physics, CAS, for financial support. We are grateful to Prof. H. J. Gao and the Shanghai Supercomputer Center and the Supercomputing Center, CNIC, CAS, for providing the substantial computational facility necessary for the theoretical calculations in this work, and to Prof. F. Naumkin of the University of Ontario Institute of Technology (UOIT) for many helpful discussions.

REFERENCES AND NOTES

1. Levine R. D.; Bernstein R. B. *Molecular Reaction Dynamics and Chemical Reactivity*; Oxford University Press: 2006; Vol. 126, pp 173–186..
2. For a review see : McNab, I. R.; Polanyi, J. C. Patterned Atomic Reaction at Surfaces. *Chem. Rev.* **2006**, *6*, 4321–4364.
3. Bernstein, J.; Davis, R. E.; Shimoni, L.; Chang, N.-L. Patterns in Hydrogen Bonding: Functionality and Graph Set Analysis in Crystals. *Angew. Chem., Int. Ed. Engl.* **1995**, *34*, 1555–1573.
4. Philip, D.; Stoddart, J. F. Self-Assembly in Natural and Unnatural Systems. *Angew. Chem. Int. Ed. Engl.* **1996**, *35*, 1155–1196.
5. Burrows, A. D. Crystal Engineering using Multiple Hydrogen Bonds. *Struct. Bonding (Berlin)* **2004**, *108*, 55–95.
6. Prints, L. J.; Timmerman, P.; Reinhoudt, D. N. Non-Covalent Synthesis of Organic Nanostructures. *Pure Appl. Chem.* **1998**, *70*, 1459–1468.
7. Patitsas, S. N.; Lopinski, G. P.; Hul'ko, O.; Moffatt, D. J.; Wolkow, R. A. Current-Induced Organic Molecule-Silicon Bond Breaking: Consequences for Molecular Devices. *Surf. Sci.* **2000**, *457*, L425–L431.
8. Lu, P. H.; Polanyi, J. C.; Roger, D. Electron-Induced Localized Atomic Reaction (LAR): Chlorobenzene Adsorbed on Si(111)-7×7. *J. Chem. Phys.* **1999**, *111*, 9905–9907.
9. Lu, P. H.; Polanyi, J. C.; Roger, D. Photo-Induced Localized Atomic Reaction (LAR) of 1,2- and 1,4-Dichlorobenzene with Si(111) 7×7. *J. Chem. Phys.* **2000**, *112*, 11005–11010.
10. Dobrin, S.; Lu, X.; Naumkin, F. Y.; Polanyi, J. C.; Yang, J. (S. Y.). Imprinting Br-atoms at Si(111) from a SAM of CH3Br(ad), with Pattern Retention. *Surf. Sci.* **2004**, *573*, L363–L368.
11. Stipe, B. C.; Rezaei, M. A.; Ho, W. Inducing and Viewing the Rotational Motion of a Single Molecule. *Science* **1998**, *279*, 1907–1909.
12. Alavi, S.; Rousseau, R.; Lopinski, G. P.; Wolkow, R. A.; Seideman, T. Controlling Organic Reactions on Silicon Surfaces with a Scanning Tunneling Microscope: Theoretical and Experimental Studies of Resonance-Mediated Desorption. *Faraday Discuss.* **2000**, *117*, 213–229.
13. Alavi, S.; Rousseau, R.; Patitsas, S. N.; Lopinski, G. P.; Wolkow, R. A.; Seideman, T. Inducing Desorption of Organic Molecules with a Scanning Tunneling Microscope: Theory and Experiments. *Phys. Rev. Lett.* **2000**, *85*, 255372–255375.
14. Lauhon, L. J.; Ho, W. Single-Molecule Chemistry and Vibrational Spectroscopy: Pyridine and Benzene on Cu(001). *J. Phys. Chem. A* **2000**, *104*, 2463–2467.
15. Ho, W. Single-Molecule Chemistry. *J. Chem. Phys.* **2002**, *117* (24), 11033–11061.
16. Komeda, T.; Kim, Y.; Fujita, Y.; Sainoo, Y.; Kawai, M. Local Chemical Reaction of Benzene on Cu(11) via STM-Induced Excitation. *J. Chem. Phys.* **2004**, *120* (11), 5347–5352.
17. Hahn, J. R.; Ho, W. Orbital Specific Chemistry: Controlling the Pathway in Single-Molecule Dissociation. *J. Chem. Phys.* **2005**, *122*, 2447041–2447043.
18. Lastapis, M.; Martin, M.; Riedel, D.; Hellner, L.; Comtet, G.; Dujardin, G. Picometer-Scale Electronic Control of Molecular Dynamics inside a Single Molecule. *Science* **2005**, *308*, 1000–1003.
19. Ohara, M.; Kim, Y.; Kawai, M. Tunneling-Electron-Induced Hopping of Methylthiolate on Cu(111). *Jpn. J. Appl. Phys.* **2006**, *45* (3B), 2022–2025.
20. Yoder, N. L.; Guisinger, N. P.; Hersam, M. C.; Jorn, R.; Kaun, C.-C.; Seideman, T. Quantifying Desorption of Saturated Hydrocarbon from Silicon with Quantum Calculations and Scanning Tunneling Microscopy. *Phys. Rev. Lett.* **2006**, *97*, 1876011–1876014.
21. Nagao, M.; Mukai, K.; Yamashita, Y.; Yoshinobu, J. The Precursor Mediated Chemisorption of Vinyl Bromide on Si(100)c(4×2). *J. Phys. Chem. B* **2004**, *108*, 5703–5708.
22. Cho, J.-H.; Kleinman, L. Dissociative Adsorption of Vinyl Bromide on Si(001): A First-Principles Study. *Phys. Rev. B* **2005**, *71*, 1253301–1253305.
23. Dobrin, S.; Harikumar, K. R.; Polanyi, J. C. STM Study of the Conformation and Reaction of Long-Chain Haloalkanes at Si(111)-7×7. *J. Phys. Chem. B* **2006**, *110*, 8010–8018.
24. Dobrin, S.; Harikumar, K. R.; Jones, R. V.; Mcnab, I. R.; Polanyi, J. C.; Waqar, Z.; Yang, J. (S. Y.). Molecular Dynamics of Haloalkane Corral Formation and Surface Halogenation at Si(111)-7×7. *J. Chem. Phys.* **2006**, *125*, 1334071–1334079.
25. Henkelman, G.; Uberuaga, B. P.; Jónsson, H. A. Climbing Image Nudged Elastic Band Method for Finding Saddle Points and Minimum Energy Paths. *J. Chem. Phys.* **2000**, *113* (22), 9901–9904.
26. Stroscio, J. A.; Celotta, R. J. Controlling the Dynamics of a Single Atom in Lateral Atom Manipulation. *Science* **2004**, *306*, 242–247.
27. Menzel, D.; Gomer, R. Desorption from Metal Surfaces by Low-Energy Electrons. *J. Chem. Phys.* **1964**, *41*, 3311–3328.
28. Redhead, P. A. Interaction of Slow Electrons with Chemisorbed Oxygen. *Can. J. Phys.* **1964**, *42*, 886–905.
29. Perdew, J. P.; Burke, K.; Ernzerhof, M. Generalized Gradient Approximation Made Simple. *Phys. Rev. Lett.* **1996**, *77* (18), 3865–3868.
30. Blöchl, P. E. Projector Augmented-Wave Method. *Phys. Rev. B* **1994**, *50* (24), 17953–17979.
31. Kresse, G.; Furthmüller, J. Efficient Iterative Schemes for Ab Initio Total-Energy Calculations using a Plane-Wave Basis Set. *Phys. Rev. B.* **1996**, *54*, 11169–11186.
32. Kresse, G.; Hafner, J. Ab Initio Molecular Dynamics for Liquid Metals. *Phys. Rev. B* **1993**, *47* (1), 558–561.